Effect of fines content on soil freezing characteristic curve of sandy soils

Quoc Hung Vu, Jean-Michel Pereira, Anh Minh Tang

Effect of fines content on soil freezing characteristic curve of sandy soils

Quoc Hung VU, Jean-Michel PEREIRA, Anh Minh TANG

Laboratoire Navier, Ecole des Ponts, Univ Gustave Eiffel, CNRS, Marne-la-Vallée, France

Corresponding author:

Dr. Anh Minh TANG

Research Director

Ecole des Ponts ParisTech

6-8 avenue Blaise Pascal

77455 Marne-la-Vallée

France

Email: anh-minh.tang@enpc.fr

Abstract: Soil freezing characteristic curve (SFCC) represents the relationship between soil temperature and unfrozen water content of soil during freezing and thawing processes. In this study, SFCC of sandy soils was determined in laboratory. Pure sand was mixed with clay at various contents (0, 5, 10, 15, and 20% of the total dry mass) and the mixtures were compacted to their respective maximum dry density. Compacted specimens were then placed in a close and rigid cell and the soil's temperature was decreased step-by-step to freeze the soil water and then increased back to thaw it. During this thermal cycle, soil's temperature and volumetric water content were monitored in order to determine the SFCC. The results show that SFCC was strongly dependent on the fines content: at higher fines content, the temperature of spontaneous nucleation was lower and the residual unfrozen volumetric water content was higher.
Keywords: temperature of spontaneous nucleation, hysteresis, soil freezing characteristic curve, residual water content.

1. Introduction

Frozen soil consists of mineral particles, liquid water, ice and gas. It is formed from unfrozen soil during freezing, when a fraction of liquid water solidifies into ice at temperatures sufficiently low below 0 °C [1]. This phase change causes significant modifications of physical-hydraulic-mechanical properties of soils [2]. The freezing-thawing process is encountered in cold regions, seasonal cold regions as well as construction works using artificial ground freezing technique. Two main consequences of this process that need to be mentioned are frost heave and thaw settlement. These phenomena can induce damages to infrastructure [3–6].

The freezing-thawing process in porous media has been investigated not only in civil engineering and geosciences but also in physics [7–11]. While bulk water melts at 0 °C, water in porous media melts at temperatures below 0 °C because of physical interactions between water and solid particles [12–14]. Freezing process of a soil sample (where heat is extracted from the sample with a constant rate) can be divided into three steps (as shown in Fig. 1): (i) supercooling with release of sensible heat; (ii) first water freezing with release of latent heat; (iii) further water freezing with release of sensible heat. In the first step, during cooling (extraction of heat from soil), soil temperature decreases to reach a certain value from that it cannot decrease anymore. This value is called temperature of spontaneous nucleation T_{sn} where the first ice embryo nucleus forms because it attains the critical size [15, 16]. Formation of ice crystals releases latent heat and thus increases soil temperature. From T_{sn}, soil temperature increases to reach another value which is called freezing temperature T_f, where it remains on a plateau for a while. During this second step, soil water is gradually frozen along with releasing latent heat. After that, within the third step, soil temperature decreases with further water freezing. Freezing temperature T_f, also considered to be equal to thawing temperature T_t at which soil state changes from frozen to unfrozen, is usually used as a boundary value index to distinguish between frozen soil and unfrozen soil [17–19]. These characteristic temperatures (T_{sn} and T_f) were investigated in several studies [15, 18, 20].

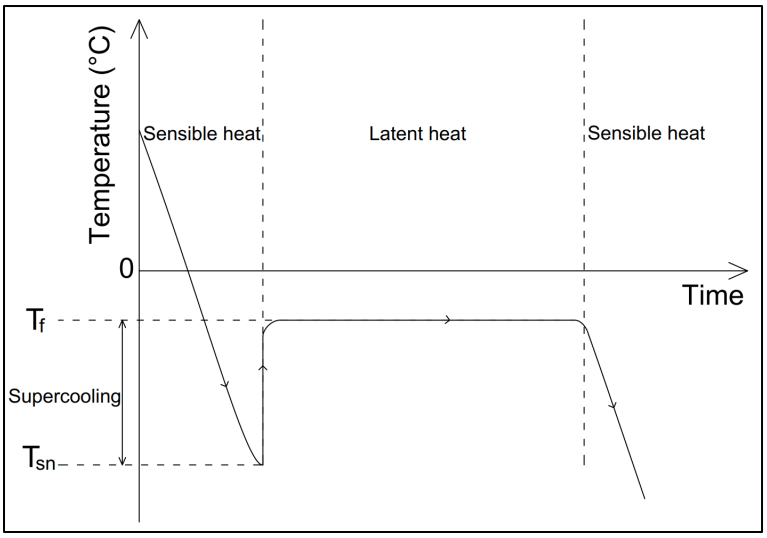

Fig. 1 Freezing process of soil-water system.

Soil freezing characteristic curve (SFCC) represents the relationship between the temperature and the quantity of liquid water in soil. It is one of the most essential data in studying the freezing-thawing process in soils. On the one hand, several SFCC models were empirically developed. From SFCC obtained experimentally, empirical models were proposed using power, piecewise or exponential functions [21–28]. On the other hand, SFCC can be derived from soil water characteristic curve (SWCC). This approach is based on the theory of similarity between freezing-thawing and drying-wetting processes that is illustrated by Clapeyron equation [29–37]. More generally, various physical models were developed based on theory of capillarity, sorption or that of interface pre-melting [38–40]. Most of the existing SFCC models consider the effect of fines content but this effect is considered in different ways. For instance, some empirical models used specific surface or liquid limit as input data while physics-based models consider absorption parameters of soil. Due to the diversity of SFCC models, there is no unified standard for choosing SFCC in numerical simulations [41]. In addition, except few models (e.g., [35]), most of the existing ones consider a unique relationship between unfrozen water content and temperature. However, this relation obtained on the freezing path can differ from that of that of the thawing path; at a given temperature, water content of the freezing path can be higher than at of the thawing path. This hysteresis is usually ignored in the models.

To determine SFCC in the laboratory, a soil specimen is usually subjected to a freeze-thaw cycle, while unfrozen water content is measured. Although controlling specimen's temperature is technically feasible, measuring unfrozen water content is much more challenging. Several methods and techniques have been developed to evaluate the unfrozen water content at negative temperature, including dilatometry [42, 43], gas dilatometry [44], adiabatic calorimetry [45, 46], isothermal calorimetry [28], differential scanning calorimetry [10, 47, 48], X-ray diffraction [49, 50], time/frequency domain reflectometry (TDR/FDR) [51–53] and pulsed nuclear magnetic resonance (P-NMR) [38, 54, 55]. Among these methods, TDR and P-NMR are the two most common ones. P-NMR is widely acknowledged as a highly accurate and non-destructive technique. However, the equipment required for this technique is generally expensive [56]. Compared to P-NMR, TDR/FDR can be used in the laboratory as well as in the field and it is cheaper, quicker, and more portable. With TDR, unfrozen water content is inferred from the measurement of apparent dielectric constant of soil using an empirical equation [57, 58] or dielectric mixing models [51, 59, 60]. It is noted that several factors such as temperature or bound water can affect its accuracy.

Several studies have determined SFCC in the laboratory in both freezing and thawing processes [18, 40, 42, 55, 61–64]. These studies recognized that hysteresis exists in SFCC in which the unfrozen water content is different in thawing and freezing processes at the same temperature. Hysteresis in freezing-thawing process was believed to be similar to that of wetting-drying process. However, the mechanism inducing hysteresis in SFCC is complex and it may be influenced by several effects such as supercooling, pore blocking, capillarity, free energy barriers, contact angles and electrolytes [55, 62]. It is also noted that hysteresis is significant at temperatures between -2 °C and 0 °C [42, 65, 66] and that it should not be ignored due to impacts on unfrozen water content on frost heaving [67, 68], creep behaviour of frozen soils [69, 70] as well as thermal regime of frozen ground [71].

Beside hysteresis effect, it is found that the shape of SFCC depends also on several factors, including liquid limit [28], stress condition [72], salt content and solute types [38, 73], initial water content or degree of saturation [74–76], types of soil [18, 62, 65], pore-size distribution [55], and fines content [18, 28, 55, 63]. Among these factors, fines content can influence others (liquid limit, pore-size distribution and types of soil). As far as fines content is concerned, by determining unfrozen water content of several clays, a silt and a gravel, Tice et al. [28] observed significantly different unfrozen water contents at the same temperature below 0 °C. Tian et al. [63] carried out tests on three soils corresponding to three clay contents and found that unfrozen water degree of saturation also changed in different ways in both freezing and thawing processes. For soils containing higher clay fraction, unfrozen water degree of saturation was higher at any given temperature below freezing point and the hysteresis loop was smaller. The same findings concerning SFCC were obtained in the study of Zhang et al. [18] on silty clay, and silt and in the study of Li et al. [55] on silty clay, fine sand, and medium sand. Some other authors also investigated different soils but the effect of fines content was out of their focus [22, 30, 54, 62].

The present study aims at systematically investigating the effect of fines content on the SFCC of sandy soils. Clean sand was mixed with clay at dry state firstly and water afterward to obtain sandy soils with clay content of 0, 5, 10, 15, and 20% prior to compaction at the Proctor maximum dry density followed by a saturation phase. The specimen's temperature was then decreased progressively to freeze the soil specimen in undrained conditions prior to applying the thawing process. During this freezing-thawing cycle, soil's temperature and unfrozen water content were measured. After the introduction, the second section of this paper presents the materials and experimental methods. Experimental results are presented in the third section, before being discussed in the fourth section.

2. Materials and experimental methods

2.1. Experimental setup

The experimental setup is shown in Fig. 2 and the details of the sensors used are presented in Table 1. Soil specimen was contained in a rigid metallic cylindrical cell (150 mm in height and 150 mm in diameter). The cell was immerged in a temperature-controlled bath (F38-EH JULABO with ±0.03 °C accuracy). Soil temperature was measured with a PT100 sensor, soil volumetric water content was measured with a ML2x Thetaprobe sensor, and soil suction was measured with a tensiometer. As Thetaprobe sensor measures soil apparent dielectric constant (K_a) which is the ratio of the dielectric permittivity of a substance to free space, soil unfrozen volumetric water content (θ_u) was estimated from measured K_a by using empirical equations of Smith and Tice [58] (1) and Topp et al. [57] (2) for frozen and unfrozen states of soil, respectively. Equation (2) was used only for the initial state (before the occurrence of freezing)

and for the final state where thawing is complete. Equation (1) is used where ice is expected to exist in soil (i.e. after the occurrence of freezing and before the completion of thawing).

$$\theta_u = -0.1458 + 3.868 \times 10^{-2} \times K_a - 8.502 \times 10^{-4} \times K_a^2 + 9.92 \times 10^{-6} \times K_a^3 \quad (1)$$

$$\theta_u = -5.3 \times 10^{-2} + 2.92 \times 10^{-2} \times K_a - 5.5 \times 10^{-4} \times K_a^2 + 4.3 \times 10^{-6} \times K_a^3 \quad (2)$$

Table 1: Properties of sensors using in freezing-thawing tests.

Measured parameters	Principle	Type	Accuracy	Range
Temperature	Resistance temperature detector	PT100	±0.03 °C	-200 to 400 °C
Volumetric unfrozen water content	Time domain reflectometry (dielectric constant)	ThetaProbe ML2x (4 rods)	0.01 m^3/m^3	0.01 to 1 m^3/m^3
Tensiometer	Piezoelectric transducer	T5x	±0.5 kPa	-160 to 100 kPa
Thermal conductivity	Transient line heat source	KD2-Prob (RK-1)	10%	0.1 to 4 W/(m.K)

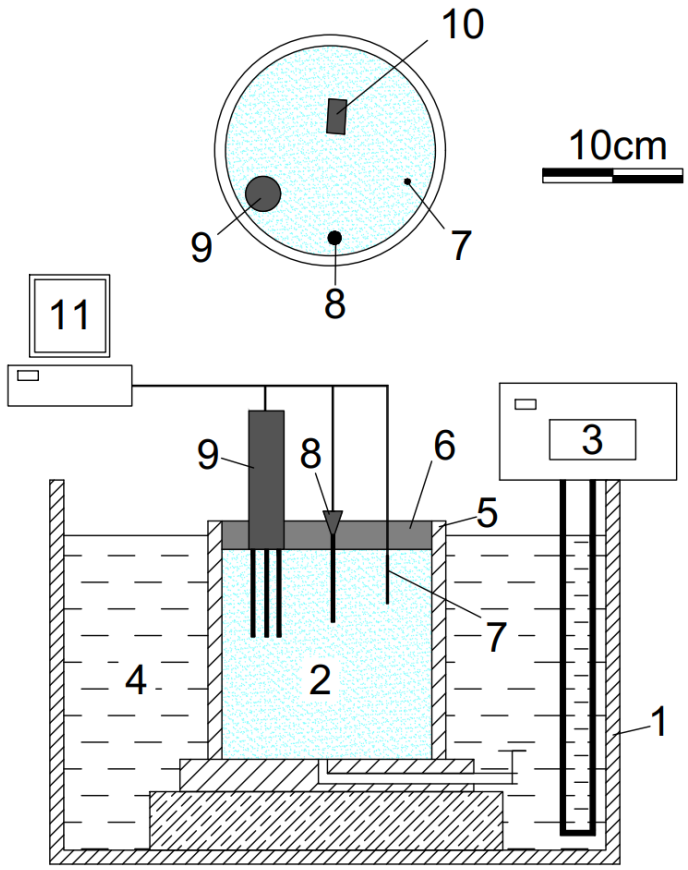

Fig. 2 Schematic view of the experimental setup. (1) Temperature-controlled bath; (2) Soil specimen; (3) Temperature controlling system; (4) Temperature-controlled liquid (30% ethylene glycol + 70% water); (5) Metallic cylindrical cell; (6) Insulating cover; (7)

147 Temperature sensor; (8) Tensiometer; (9) Soil water sensor; (10) Thermal conductivity probe
148 (results are not presented in this study); (11) Data logger system.

149 **2.2. Material**

150 Fontainebleau sand was carefully mixed with Speswhite kaolin clay at dry state using an
151 automatic mortar mixer in order to obtain sandy soils with fines content (dry mass of clay
152 divided by dry mass of soil) of 0, 5, 10, 15, and 20%. The physical properties of sand and clay
153 are shown in Table 2 and Table 3, respectively. Fig. 3 presents the grain size distribution of
154 these soils. In this study, the name of each soil corresponds to its clay content (for instance, S10
155 corresponds to a soil having 10% of clay in dry mass). Prior to the preparation of the soil
156 specimens, each soil was carefully mixed with distilled water using the mortar mixer to obtain
157 optimum water content (determined from the Normal Proctor compaction curves obtained on
158 the same soils [77]). Afterward, wet soil was packed in a plastic bag for at least 24 h to ensure
159 the homogenisation of water content, prior to compaction in the cylindrical cell to reach its
160 maximum dry density.

161 Table 2. Physical properties of sand.

Property	**Value**
Median grain size, D_{50} (mm)	0.21
Uniformity coefficient, C_U	1.52
Minimum void ratio, e_{min}	0.54
Maximum void ratio, e_{max}	0.94
Particle density, ρ_s (Mg/m^3)	2.65
Minimum dry density, $\rho_{d,min}$ (Mg/m^3)	1.37
Maximum dry density, $\rho_{d,max}$ (Mg/m^3)	1.72

162 Table 3: Physical properties of clay.

Property	**Value**
Liquid limit, LL (%)	55
Plastic limit, PL (%)	30
Plasticity index, PI	25
Specific surface area (m^2/g)	0.94
Particle density, ρ_s (Mg/m^3)	2.65
Particle diameter < 0.002 mm (%)	79
Particle diameter > 0.01 mm (%)	0.5
Maximum dry density, $\rho_{d,max}$ (Mg/m^3)	1.45

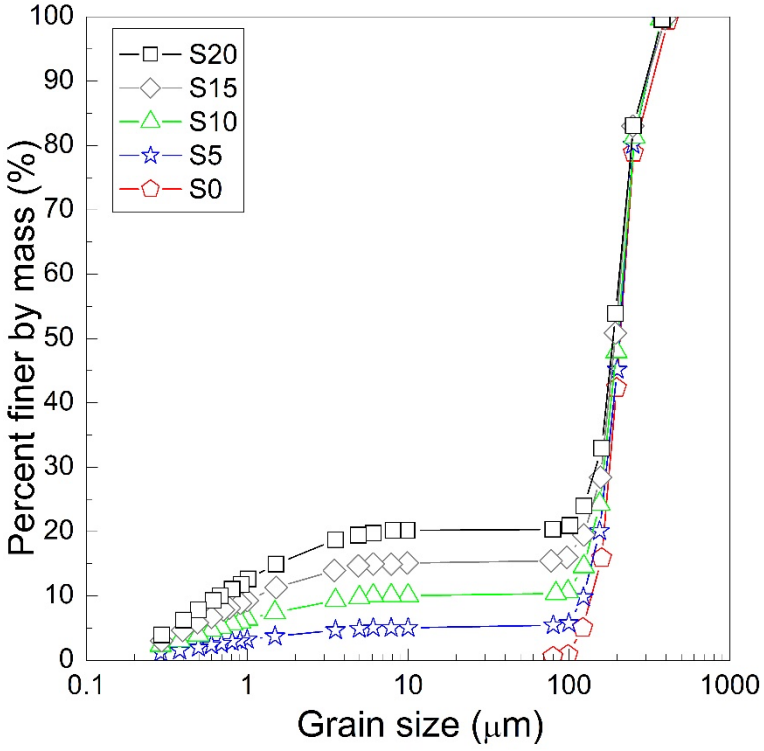

163

164 **Fig. 3** Grain size distribution curves.

165 **2.3. Experimental procedure**

166 After soil compaction in the cell, sensors were installed as shown in Fig. 2 and an insulating
167 cover made of expanded polystyrene was placed in order to avoid heat exchange between soil
168 specimen and ambient air. The whole system was then transferred inside the temperature-
169 controlled bath. Prior to the freezing-thawing test, soil specimen was saturated by injecting
170 water from the bottom of the specimen during 0.5 to 2 days depending on fines content. After
171 the saturation (when a layer of water of 10 mm was visible on the top of the specimen), the
172 temperature of the bath was first set at a temperature between 0 °C and -1 °C (slightly higher
173 than the expected T_{sn}). Each test started with the cooling path. The bath temperature was
174 decreased in steps of 0.1 °C to freeze the soil pore water. Once the freezing was triggered, the
175 temperature continued to be decreased in steps of 0.2 °C until -2 °C or -3 °C to observe the
176 change of liquid water content during further cooling. Afterward, during the heating path, the
177 bath temperature was increased in steps of 0.2 °C until 0 °C to thaw the frozen soil. During both
178 cooling and heating paths, the bath temperature was changed to the subsequent step only when
179 soil temperature and volumetric unfrozen water content (measured by the sensors) had reached
180 their equilibrium state. The equilibrium state was considered reached when these two quantities
181 did not change (< 0.05 °C for temperature and < 1% for water content) during at least 2 h.

182 The test program is shown in Table 4. The test number shows the soil tested (S0 to S20)
183 followed by the number of replicate test (T1 to T4). At least two tests were performed for each
184 soil. Tests T1 were performed following the procedure described above to obtain the complete
185 SFCC curves. For the other tests (T2, T3, T4), only the freezing path of the same procedure was
186 performed in order to replicate the characteristic temperatures.

187 Table 4: Physical properties of soils.

Test No.	Fines content (%)	Dry density (Mg/m^3)	Porosity (-)	Test duration (h)
S20-T1	20	1.98	0.25	754
S20-T2	20	1.96	0.26	26
S15-T1	15	1.99	0.25	712
S15-T2	15	2.00	0.25	64
S10-T1	10	1.91	0.28	590
S10-T2	10	1.90	0.28	153
S5-T1	5	1.78	0.33	817
S5-T2	5	1.78	0.33	143
S5-T3	5	1.78	0.33	190
S0-T1	0	1.67	0.37	756
S0-T2	0	1.67	0.37	286
S0-T3	0	1.67	0.37	75
S0-T4	0	1.68	0.37	187

3. Experimental results

3.1. Typical test (S10-T1)

As an example, the results of test S10-T1 are shown in Fig. 4 where soil temperature, suction, and volumetric unfrozen water content are plotted versus elapsed time for the cooling path.

From -1.2 °C, soil temperature was decreased in steps of 0.1 °C down to -1.6 °C. During this period, soil temperature was controlled through the bath's temperature, suction remained equal to zero and volumetric water content remained constant. When soil temperature reached -1.6 °C, soil freezing started inducing abrupt changes in the three measured quantities. Results obtained during this stage (elapsed time of 70 – 86 h) are shown in Figure 5 for a better view.

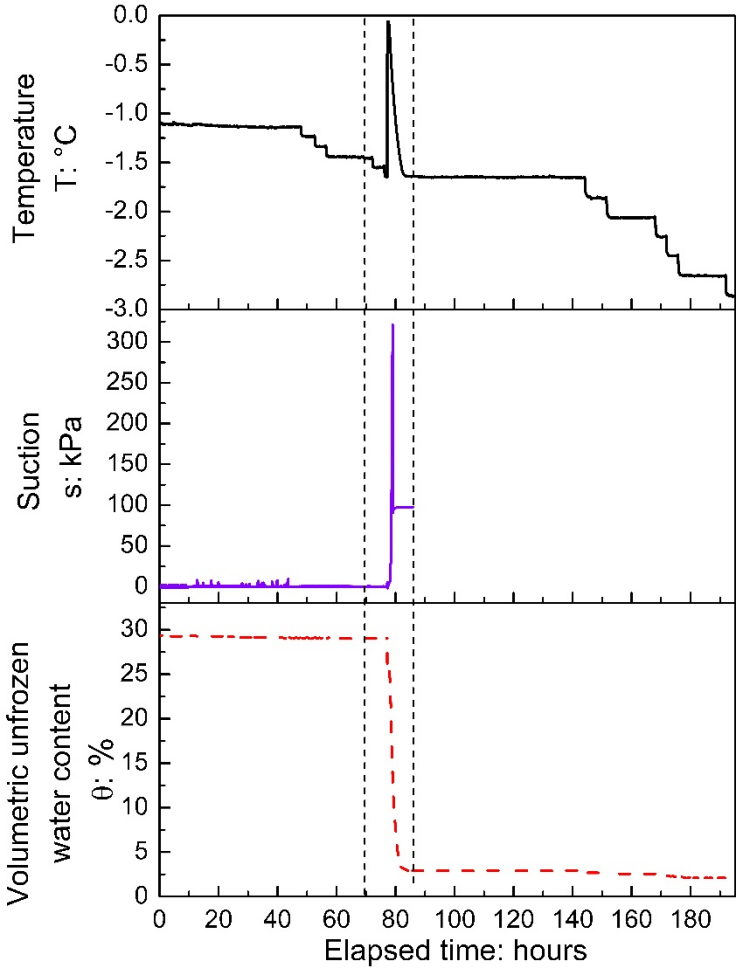

197

198 **Fig. 4** Soil temperature, volumetric unfrozen water content and suction versus elapsed time
199 during the cooling path of test S10-T1.

200 As shown in Fig. 5, when the bath temperature was changed from -1.5 °C to -1.6 °C (at 76 h),
201 soil temperature changed to -1.6 °C after a few minutes. At 77 h, while the bath temperature
202 was still maintained at -1.6 °C, soil temperature increased abruptly to -0.1 °C prior to a
203 progressive decrease and reached the imposed temperature (-1.6 °C) again at 83 h. Soil suction
204 started to increase at 78 h and reached a maximum value of 300 kPa prior to fall down to 100
205 kPa. At 77 h, soil water content decreased abruptly from 28% to 26% prior to decrease
206 progressively to 3 % at 82 h. These results are representative of a freezing process in soil (Fig.
207 1) where the phase before 77 h corresponds to the supercooling step. At 77 h, soil water started
208 to freeze: soil temperature increased abruptly because of latent heat release prior to decrease
209 because of heat diffusion toward the liquid surrounding the cell; soil suction increased quickly
210 because of the cryogenic suction induced by ice formation in the pore space (the sudden
211 decrease of suction from 300 kPa to 100 kPa corresponded to the cavitation of the tensiometer,
212 after this moment, the sensor did not provide anymore the real soil suction); volumetric water
213 content decreased because of ice formation. From these typical results, the following parameters
214 were defined to characterise the freezing process (see Figure 5): (i) temperature of spontaneous
215 nucleation, T_{sn}; (ii) freezing point, T_f; (iii) residual volumetric unfrozen water content, θ_r (the
216 value recorded at temperature equal to T_{sn}) ; (iv) duration of the temperature plateau, t_p; (v)
217 duration of the freezing process, t_f.

After the freezing process (from 83 h), decrease of temperature induced slight decrease of volumetric unfrozen water content (see Figure 4) while soil suction measurement was no longer available because of the cavitation of the tensiometer.

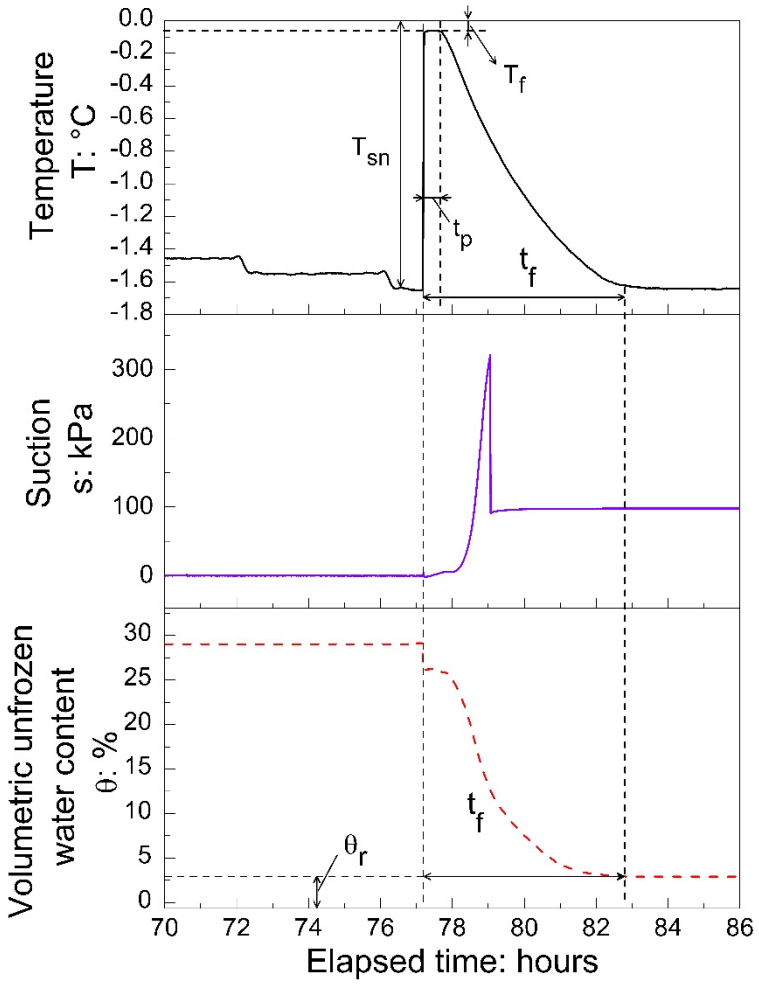

Fig. 5 Soil temperature, volumetric unfrozen water content and suction versus elapsed time during the freezing process of test S10-T1 (detailed view from 70h to 86 h).

Fig. 6 shows the results of test S10-T1 during the heating path. During this path, temperature was increased by steps of 0.2 °C from -2.8 °C to 0 °C. It induced thawing of frozen water (corresponding to a gradual increase of unfrozen water content).

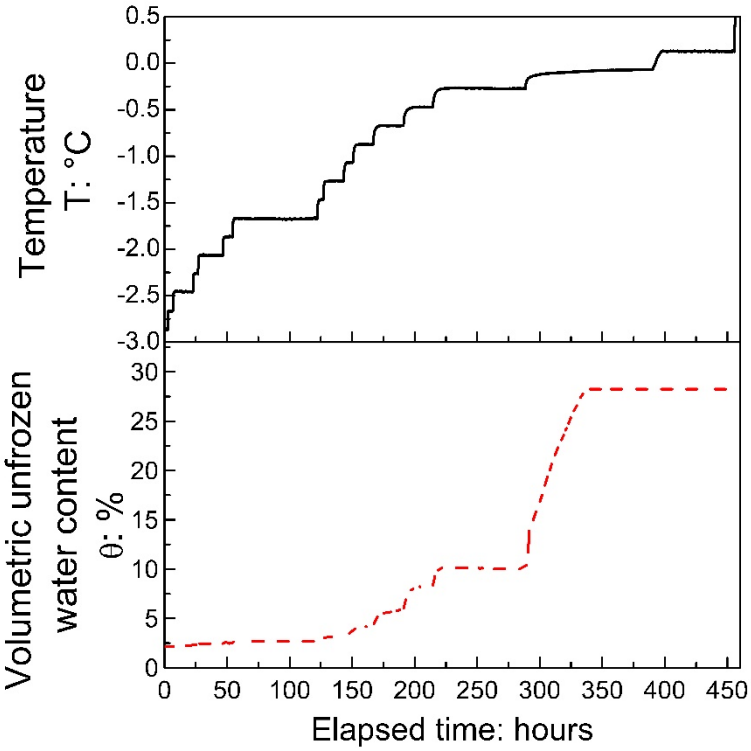

227

228 **Fig. 6** Soil temperature and volumetric unfrozen water content versus elapsed time during the
229 heating path of test S10-T1.

230 From the results shown in Fig. 4, Fig. 5 and Fig. 6, volumetric unfrozen water content obtained
231 at the end of each step is plotted versus the corresponding soil temperature for test S10-T1 in
232 Fig. 7. These results correspond to the SFCC of soil S10 obtained from test S10-T1, which
233 include both freezing and thawing paths.

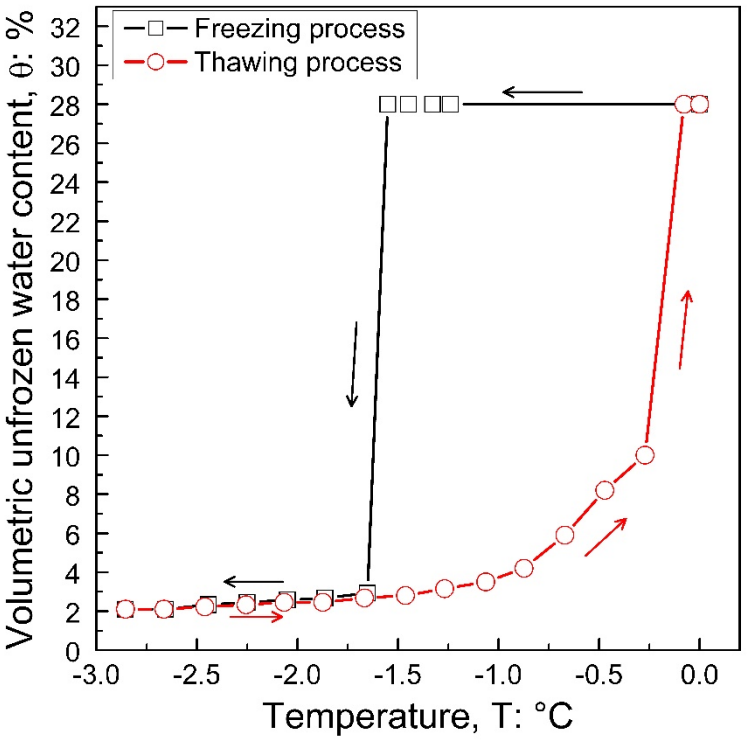

234

Fig. 7 Soil freezing characteristic curve determined from test S10-T1.

3.2. Effects of fines content

SFCC of all soils are shown in Fig. 8 where volumetric unfrozen water content was plotted versus temperature. As the initial volumetric water content (which depends on soil dry density) was different from one soil to the others, it is thus difficult to analyse the effect of fines content from these results. For this reason, volumetric unfrozen water content was used to calculate unfrozen water degree of saturation ($S_r = \theta/\theta_{sat}$; where θ_{sat} is the volumetric unfrozen water content at saturate state). Fig. 9 shows SFCC of all soils where unfrozen degree of saturation was plotted versus temperature. For each soil, from the initial saturated state, when soil temperature decreased from 0 °C, soil remained saturated with unfrozen water. When temperature reached the temperature of spontaneous nucleation, freezing was triggered inducing significant decrease of unfrozen water degree of saturation. After this step, cooling induced only slight decrease of unfrozen water degree of saturation. During the heating path, unfrozen water degree of saturation increased gradually with temperature and the relationship between these two quantities was significantly different from the cooling path for all soils.

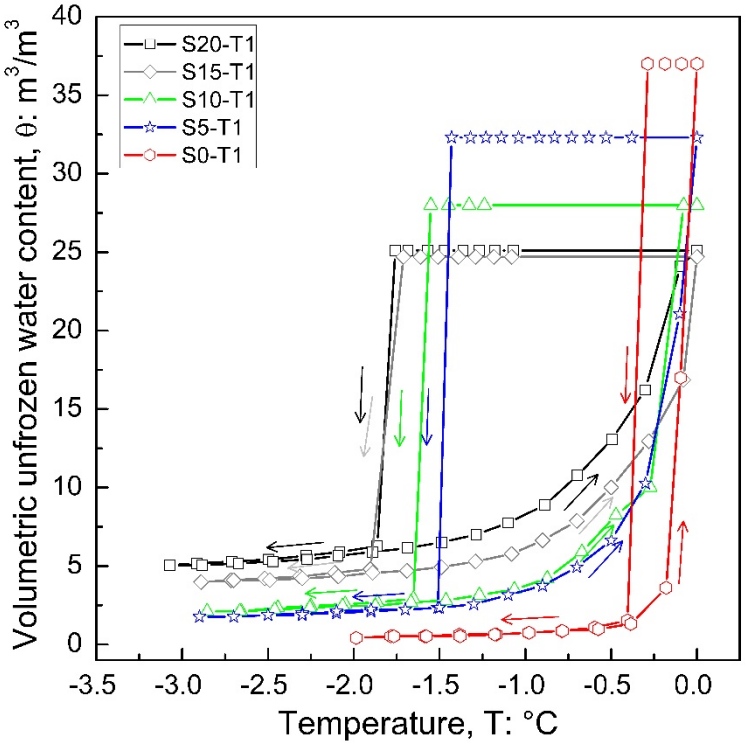

Fig. 8 Soil freezing characteristic curve (volumetric unfrozen water content versus temperature) for all soils.

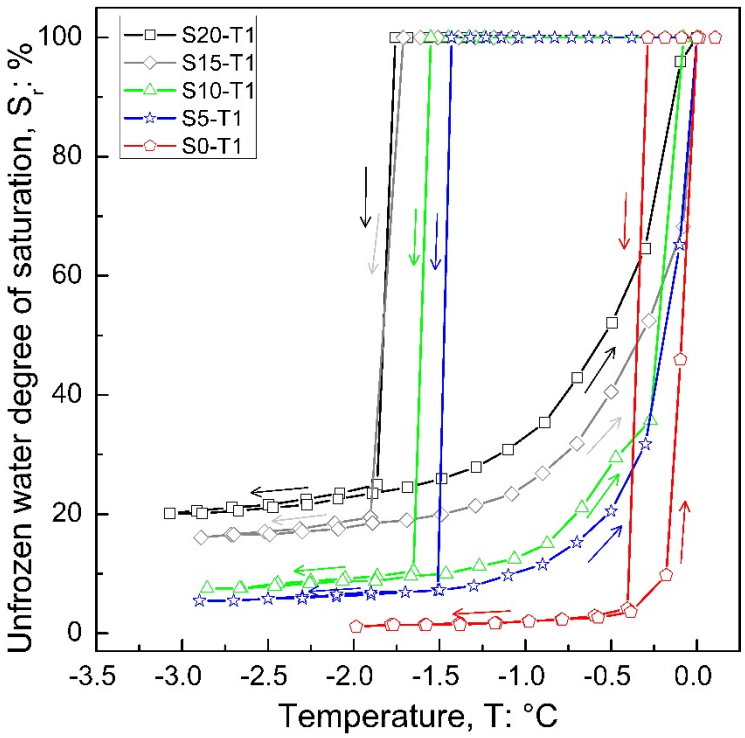

Fig. 9 Soil freezing characteristic curve (unfrozen water degree of saturation versus temperature) for all soils.

In order to quantitatively assess the effects of fines content, temperatures of spontaneous nucleation T_{sn} and freezing point T_f were plotted versus fines content (Fig. 10). The results show that the temperature of freezing point was close to 0 °C for all soils. The results were quite repeatable (with variation less than 0.1 °C) and only a slight trend of decrease of T_f when fines content increase could be observed. For T_{sn}, results showed a higher scattering (up to 0.5 °C, except for test at 0% of clay content where this value varied from -0.4 °C to -1.5 °C). In general, T_{sn} is lower at a higher clay content.

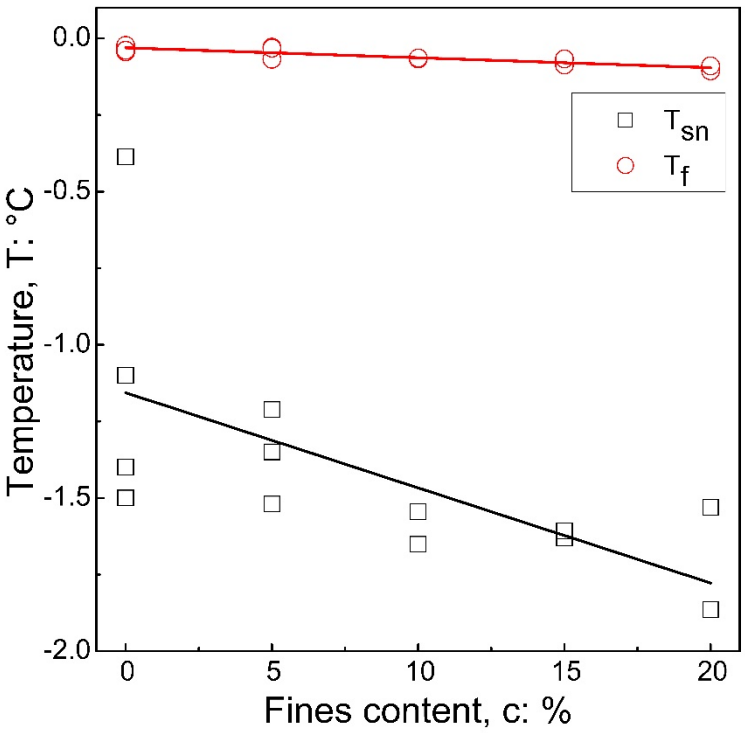

264

265 **Fig. 10** Temperatures of spontaneous nucleation and freezing point versus fines content

266 Fig. 11 shows the residual unfrozen water content θ_r (the value determined at a temperature
267 equal to T_{sn} , see Fig. 5) versus fines content. A good repeatability (with a scattering of 0.5 %)
268 could be observed. The results show that residual unfrozen water content was higher at a higher
269 fines content.

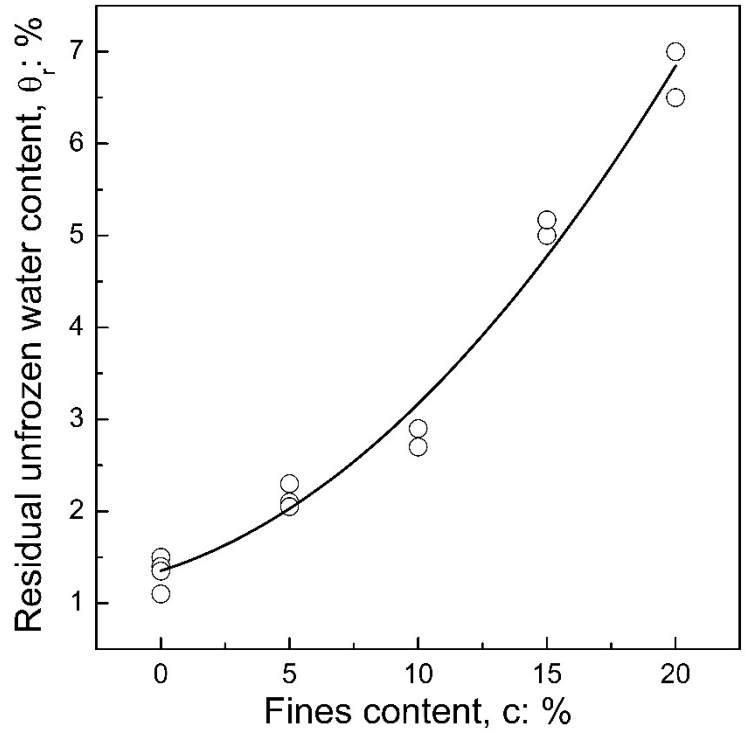

270

Fig. 11 Residual unfrozen water content versus fines content.

Fig. 12 presents the duration of the temperature plateau t_p and the duration of the freezing process t_f (see the definition on Fig. 5) versus fines content. Results of t_p were quite scattering for 0 and 5% of fines content, varying from 0.80 to 4.40 h. They were more repeatable at higher fines contents. A general decrease of this duration when the fines contents increased could be observed. Results of t_f varied between 5 and 10 h (except one test, S0-T1 where it was very long, 37.50 h). These results did not show any clear trend.

Table 5 shows the obtained characteristic parameters of all tests for better comparison.

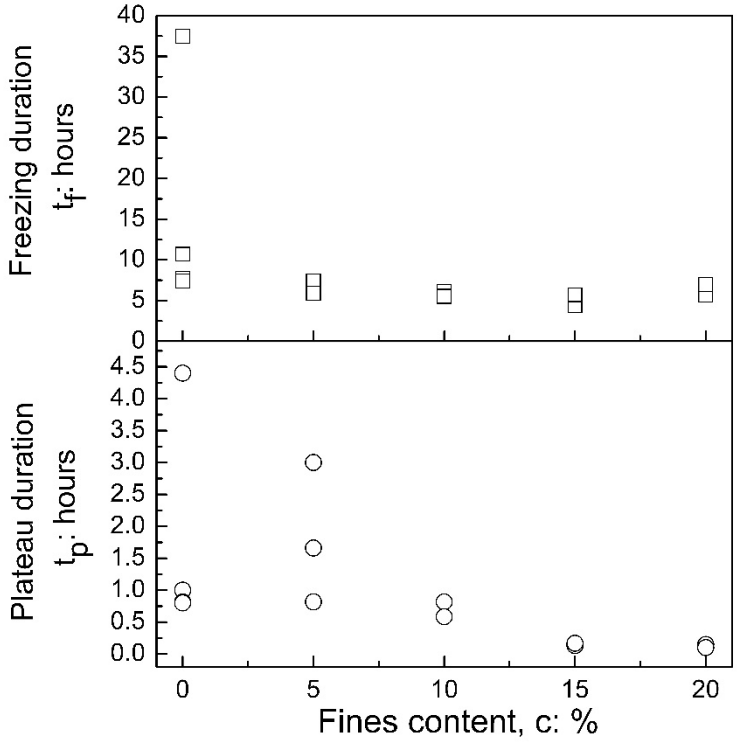

Fig. 12 Duration of the temperature plateau and duration of the freezing process versus fines content.

Table 5: Summary of characteristic parameters in freezing of tests

Test No.	Fines content (%)	T_{sn} (°C)	T_f (°C)	θ_r (-)	t_p (h)	t_f (h)
S20-T1	20	-1.86	-0.11	6.5	0.15	5.65
S20-T2	20	-1.53	-0.09	7.0	0.10	6.95
S15-T1	15	-1.61	-0.07	5.2	0.17	5.70
S15-T2	15	-1.63	-0.09	5.0	0.13	4.00
S10-T1	10	-1.65	-0.07	2.9	0.58	5.50
S10-T2	10	-1.55	-0.06	2.7	0.80	6.10

S5-T1	5	-1.52	-0.03	2.3	0.82	5.90
S5-T2	5	-1.21	-0.07	2.1	3.10	7.35
S5-T3	5	-1.35	-0.03	2.1	1.70	7.40
S0-T1	0	-0.39	-0.04	1.5	4.40	37.50
S0-T2	0	-1.51	-0.02	1.10	1.00	7.70
S0-T3	0	-1.10	-0.04	1.40	0.80	10.70
S0-T4	0	-1.40	-0.02	1.35	0.80	7.40

4. Discussion

In this study, in order to determine the relationship between unfrozen water content and temperature during a freezing-thawing cycle, large soil specimens (150 mm in height and 150 mm in diameter) were prepared in order to embed several sensors within the soil mass. To minimise thermal and any other gradients, soil temperature was changed by small steps and equilibrium was checked at the end of each step prior the subsequent step. At equilibrium, the soil temperature and unfrozen water content were thus supposed to be homogeneous within the specimen. Similar large soil specimens were equally used in previous studies investigating SFCC with TDR method for measurement of unfrozen water content [18, 53, 75, 78]. Smaller specimens were used when measurements were performed by pulsed-NMR method [30, 63, 79]. In several previous works, specimens were immerged in a cooling bath with constant cooling rate or at low temperature (between -15 °C and -30 °C) and kept for several hours [17, 73, 80, 81]. For determining SFCC, unfrozen water content was measured at various controlled temperatures [18, 53, 75, 76, 78, 79]. The difference between two successive controlled temperatures in these studies varies between 0.3 °C and 5 °C. In the present work, temperature steps of 0.1 °C and 0.2 °C were chosen before the occurrence of freezing phenomenon and afterward, respectively, in order to determine more accurately the freezing point, the temperature of spontaneous nucleation and the SFCC.

The measurement of unfrozen water content in the present study was converted from the measurement of apparent dielectric constant. In this study, under the influence of temperature, dielectric constant of each phase in soils changes, particularly those of water and ice [82, 83]. Several models exist to estimate moisture content from unfrozen soil apparent dielectric constant [51, 53, 57–60, 84–86]. The most used is Topp's empirical model [57] but it is not compatible with frozen soils [44, 58, 87]. Otherwise, Smith and Tice [58] proposed a model based on comparison of unfrozen water content measured from NMR and TDR methods for 25 soils covering a wide range of specific surface areas. For this reason, in the present work, the model of Smith and Tice [58], which provides an accuracy of ±3% compared to measurements from NMR method, was used for frozen soils.

Hysteresis of SFCC (difference between the freezing and the thawing curves) is usually attributed to the same factors inducing hysteresis in SWCC, such as the effect of electrolytes, pore geometry, pore blocking, effect of contact angle and change in pore structure [78]. Actually, in a freezing process, increasing solute concentration by forming ice from water increases the effect of electrolyte. Otherwise, forming ice also changes soil skeleton that affects matric potentials of soils. In addition, the hysteric behaviour is also mainly attributed to supercooling of pore water [18, 54, 62, 63]. Instead of freezing at 0 °C, pore water is necessarily supercooled at lower temperature. In the present work, an insignificant hysteresis of θ_u was

observed for all soils below T_{sn} (at frozen state). First, the effect of electrolytes can be ignored. Second, temperature below T_{sn} of -1 °C to -2 °C corresponds to a suction of 1 MPa to 2.5 MPa following the Clapeyron equation. This high range of suction corresponds mainly to water in micropore (intra-aggregates) in the clay matrix where SWCC is also reversible. As a result, hysteresis of SFCC observed in the present work could be contributed mainly to supercooling. After the triggering of freezing, SFCC obtained at temperature lower than T_{sn} were generally reversible (see Fig. 8 & Fig. 9).

Results shown in Fig. 9 demonstrate significant effect of fines content on the thawing path of SFCC; at a given temperature, a higher unfrozen water degree of saturation was obtained at a higher fines content. These results are consistent with the findings of previous works [28, 55, 63, 70]. Following these studies, Gibbs-Thompson equation can be used to relate the pore size distribution and the thawing path of SFCC; a lower temperature corresponds to a smaller pore. In the present work, soil having higher fines content would have a larger volume of micropores (inter-aggregates and intra-aggregates pores) a lower volume of macropores (space between sand particles).

T_{sn} determined in this study can be associated to supercooling. Fig. 10 shows that this parameter generally decreased with an increase of fines content and it was measured with a relatively high scattering. For bulk water, T_{sn} depend on numerous factors such as sample volume, cooling velocity, the presence and concentration of solutes, the presence of solid impurities, effects of external fields (impulse waves, electromagnetic radiation, etc.) [9, 89, 90]. In the case of soils, additional factors can be soil components and their fractions. Many studies determined T_{sn} of various soils and found that increasing clay content in soils decreases temperature of spontaneous nucleation to lower range [15, 18]. These studies focused on clays or clay and silt and these results agree with sandy soils in the present study. It is noted that the supercooling is considered as a necessary phase to activate nucleation process and it appears in both cases, either in free pure water or within the porous volume of soils. Because of the high value of released latent heat, about 334 J/g, which appears during nucleation process, water needs to be supercooled at T_{sn} for equilibrating energy before crystallization. According to Yershov [91], T_{sn} is remarked as the temperature at which embryo nuclei form and grow to the critical sizes, about 472 H_2O corresponding to 10^{-26} m^3. The relatively high scattering of results obtained in the present work can be thus explained by the random behaviour of the crystallization process. The slight effect of fines content on T_{sn} can be explained by the effect of soil pore size distribution on the supercooling: soil having a higher fines content would have higher volume of micropores, and T_{sn} is generally lower in a smaller pore.

Numerous studies investigated T_f and showed that T_f depends on many factors such as salt content [20, 73, 80, 92, 93], salt types [17, 81], initial water content [15], soil types [10, 18, 30, 55, 94, 95], etc. In the present study, T_f was found close to 0 °C for all soils. This result can be explained by two main reasons: soils were studied at saturated state and fines content is sufficiently low. Bing and Ma [81] obtained similar results with saturated sandy soil containing less than 7.5% of clay. Furthermore, freezing point remains constant also above a certain value of water content for all soils [9, 81, 96]. Actually, for the soils considered in the present study, with relatively low contents of low plasticity kaolin clay, the amount of bound water should be negligible and T_f should be similar to that of bulk pure water, i.e. close to 0 °C.

Residual unfrozen content was found higher at a higher fines content (Fig. 11). It is believed that residual unfrozen relates almost directly to the amount of specific surface of soils. According to several studies [18, 28, 30, 55, 63], unfrozen water content remaining in soils at

the same temperature decreased in the following order: clay, silts, sands and gravel. Following Bing and Ma [81], only free water was frozen when freezing is triggered. Unfrozen water should then correspond to bound water. According to Tian et al. [63], the amount of bound water in soils is proportional to the thickness of the electric double layer and specific surface area. In the present study, a higher fines content corresponds to a higher specific surface area and then a higher amount of bound water.

The duration of temperature plateau, t_p, would depend then on the amount of latent heat released when freezing is triggered. This amount mainly depends on $T_{sn,}$ as shown in Table 5. As the results of T_{sn} show significant scattering and a general slight increase when fines content increased (Fig. 10), similar trends were observed with t_p (Fig. 12). The duration of the freezing process, t_f, which is much longer than t_p, correspond to the thermal diffusion of latent heat released during the whole freezing process. This duration would depend thus mainly on the thermal diffusivity of the frozen soil (which at the same time evolves during freezing).

5. Conclusions

The results obtained in this study show that fines content in sandy soils significantly influenced the soil behaviour under a freezing-thawing cycle. Based on the investigation of five levels of fines content (varying from 0 to 20 %), the following conclusions can be addressed:

- When the temperature decreased from 0°C, freezing was triggered at T_{sn} inducing a sudden decrease of θ_u from the saturated state to the residual state. Afterward, θ_u continued to decrease but with a lower rate. The subsequent heating induced an increase of θ_u (which represents a progressive melting of frozen water).
- The thawing path of SFCC was strongly dependent on the fines content; at a given temperature, a higher θ_u was observed for a higher fines content.
- T_{sn} was higher at a higher fines content and varied between -1.0 °C and -2.0 °C.
- T_f varied between 0°C and -0.2 °C, only a slight decrease of T_f with an increase of fines content was observed.
- θ_r (varied from 1 % to 7 %) was higher at a higher fines content.
- t_p was found scattering and slightly decreased when fines content increased.
- t_f was found independent of fines content.

The findings of the present study would be helpful to predict the soil behaviour under freezing-thawing process. That would imply several applications in cold regions and also in geotechnical engineering ground improvement by artificial ground freezing.

Data availability

The datasets generated during and/or analysed during the current study are available from the corresponding author on reasonable request.

References

1. Andersland OB, Ladanyi B (1994) An Introduction to Frozen Ground Engineering. Springer Science & Business Media

406 2. Andersland OB, Ladanyi B (2004) Frozen Ground Engineering. John Wiley & Sons

407 3. Russo G, Corbo A, Cavuoto F, Autuori S (2015) Artificial Ground Freezing to excavate
408 a tunnel in sandy soil. Measurements and back analysis. Tunn Undergr Sp Technol
409 50:226–238. https://doi.org/10.1016/j.tust.2015.07.008

410 4. Han L, Ye G, Li Y, et al (2016) In situ monitoring of frost heave pressure during cross
411 passage construction using ground-freezing method. Can Geotech J 53:530–539.
412 https://doi.org/10.1139/cgj-2014-0486

413 5. Zhang S, Sheng D, Zhao G, et al (2016) Analysis of frost heave mechanisms in a high-
414 speed railway embankment. Can Geotech J 53:520–529. https://doi.org/10.1139/cgj-
415 2014-0456

416 6. Yu W, Zhang T, Lu Y, et al (2020) Engineering risk analysis in cold regions: State of
417 the art and perspectives. Cold Reg Sci Technol 171:102963.
418 https://doi.org/10.1016/j.coldregions.2019.102963

419 7. Akyurt M, Zaki G, Habeebullah B (2002) Freezing phenomena in ice–water systems.
420 Energy Convers Manag 43:1773–1789. https://doi.org/10.1016/S0196-8904(01)00129-
421 7

422 8. Chen SL, Lee TS (1998) A study of supercooling phenomenon and freezing probability
423 of water inside horizontal cylinders. Int J Heat Mass Transf 41:769–783.
424 https://doi.org/10.1016/S0017-9310(97)00134-8

425 9. Kozlowski T (2009) Some factors affecting supercooling and the equilibrium freezing
426 point in soil–water systems. Cold Reg Sci Technol 59:25–33.
427 https://doi.org/10.1016/j.coldregions.2009.05.009

428 10. Kozlowski T (2004) Soil freezing point as obtained on melting. Cold Reg Sci Technol
429 38:93–101. https://doi.org/10.1016/j.coldregions.2003.09.001

430 11. Mishima O, Stanley HE (1998) The relationship between liquid, supercooled and glassy
431 water. Nature 396:329–335. https://doi.org/10.1038/24540

432 12. Enninful HRNB, Schneider D, Kohns R, et al (2020) A novel approach for advanced
433 thermoporometry characterization of mesoporous solids: Transition kernels and the
434 serially connected pore model. Microporous Mesoporous Mater 309:110534.
435 https://doi.org/10.1016/j.micromeso.2020.110534

436 13. Schreiber A, Ketelsen I, Findenegg GH (2001) Melting and freezing of water in ordered
437 mesoporous silica materials. Phys Chem Chem Phys 3:1185–1195.
438 https://doi.org/10.1039/b010086m

439 14. Petrov O, Furó I (2006) Curvature-dependent metastability of the solid phase and the
440 freezing-melting hysteresis in pores. Phys Rev E 73:011608.
441 https://doi.org/10.1103/PhysRevE.73.011608

442 15. Anderson DM (1968) Undercooling, freezing point depression, and ice nucleation of soil

443 water. Isr J Chem 6:349–355. https://doi.org/10.1002/ijch.196800044

444 16. ANDERSON DM (1967) Ice nucleation and the substrate-ice interface. Nature 216:563–
445 566. https://doi.org/10.1038/216563a0

446 17. Wan X, Lai Y, Wang C (2015) Experimental study on the freezing temperatures of saline
447 silty soils. Permafr Periglac Process 26:175–187. https://doi.org/10.1002/ppp.1837

448 18. Zhang M, Zhang X, Lai Y, et al (2020) Variations of the temperatures and volumetric
449 unfrozen water contents of fine-grained soils during a freezing–thawing process. Acta
450 Geotech 15:595–601. https://doi.org/10.1007/s11440-018-0720-z

451 19. Yu F, Guo P, Na S (2022) A framework for constructing elasto-plastic constitutive
452 models for frozen and unfrozen soils. Int J Numer Anal Methods Geomech 46:436–466.
453 https://doi.org/10.1002/nag.3306

454 20. Ayers AD, Campell RB (1951) Freezing point of water in a soil as related to salt and
455 moisture contents of the soil. Soil Sci 72:201–206

456 21. He Z, Teng J, Yang Z, et al (2020) An analysis of vapour transfer in unsaturated freezing
457 soils. Cold Reg Sci Technol 169:102914.
458 https://doi.org/10.1016/j.coldregions.2019.102914

459 22. Teng J, Zhong Y, Zhang S, Sheng D (2021) A mathematic model for the soil freezing
460 characteristic curve: the roles of adsorption and capillarity. Cold Reg Sci Technol
461 181:103178. https://doi.org/10.1016/j.coldregions.2020.103178

462 23. Anderson DM, Tice AR (1972) Predicting unfrozen water contents in frozen soils from
463 surface area measurements. Highw Res Rec 393:12–18

464 24. Kozlowski T (2007) A semi-empirical model for phase composition of water in clay–
465 water systems. Cold Reg Sci Technol 49:226–236.
466 https://doi.org/10.1016/j.coldregions.2007.03.013

467 25. Kozlowski T, Nartowska E (2013) Unfrozen Water Content in Representative Bentonites
468 of Different Origin Subjected to Cyclic Freezing and Thawing. Vadose Zo J 12:.
469 https://doi.org/10.2136/vzj2012.0057

470 26. Ye M, Pan F, Wu Y-S, et al (2007) Assessment of radionuclide transport uncertainty in
471 the unsaturated zone of Yucca Mountain. Adv Water Resour 30:118–134.
472 https://doi.org/10.1016/j.advwatres.2006.03.005

473 27. Ge S, McKenzie J, Voss C, Wu Q (2011) Exchange of groundwater and surface-water
474 mediated by permafrost response to seasonal and long term air temperature variation.
475 Geophys Res Lett 38:1–6. https://doi.org/10.1029/2011GL047911

476 28. Tice AR, Anderson DM, Banin A (1976) The prediction of unfrozen water contents in
477 frozen soils from liquid limit determinations. Department of Defense, Army, Corps of
478 Engineers, Cold Regions Research and Engineering Laboratory

29. Dall'Amico M (2010) Coupled water and heat transfer in permafrost modeling. University of Trento

30. Teng J, Kou J, Yan X, et al (2020) Parameterization of soil freezing characteristic curve for unsaturated soils. Cold Reg Sci Technol 170:102928. https://doi.org/10.1016/j.coldregions.2019.102928

31. Zhang X, Sun SF, Xue Y (2007) Development and Testing of a Frozen Soil Parameterization for Cold Region Studies. J Hydrometeorol 8:690–701. https://doi.org/10.1175/JHM605.1

32. Sheshukov AY, Nieber JL (2011) One-dimensional freezing of nonheaving unsaturated soils: Model formulation and similarity solution. Water Resour Res 47:1–17. https://doi.org/10.1029/2011WR010512

33. Liu Z, Yu X (Bill) (2013) Physically Based Equation for Phase Composition Curve of Frozen Soils. Transp Res Rec J Transp Res Board 2349:93–99. https://doi.org/10.3141/2349-11

34. Zhang S, Teng J, He Z, et al (2016) Canopy effect caused by vapour transfer in covered freezing soils. Géotechnique 66:927–940. https://doi.org/10.1680/jgeot.16.P.016

35. Zhou Y, Zhou J, Shi X, Zhou G (2019) Practical models describing hysteresis behavior of unfrozen water in frozen soil based on similarity analysis. Cold Reg Sci Technol 157:215–223. https://doi.org/10.1016/j.coldregions.2018.11.002

36. Sun K, Zhou A (2021) A multisurface elastoplastic model for frozen soil. Acta Geotech 16:3401–3424. https://doi.org/10.1007/s11440-021-01391-7

37. Kebria MM, Na S, Yu F (2022) An algorithmic framework for computational estimation of soil freezing characteristic curves. Int J Numer Anal Methods Geomech 46:1544–1565. https://doi.org/10.1002/nag.3356

38. Watanabe K, Mizoguchi M (2002) Amount of unfrozen water in frozen porous media saturated with solution. Cold Reg Sci Technol 34:103–110. https://doi.org/10.1016/S0165-232X(01)00063-5

39. Zhou J, Wei C, Lai Y, et al (2018) Application of the Generalized Clapeyron Equation to Freezing Point Depression and Unfrozen Water Content. Water Resour Res 54:9412–9431. https://doi.org/10.1029/2018WR023221

40. Ishizaki T, Maruyama M, Furukawa Y, Dash J (1996) Premelting of ice in porous silica glass. J Cryst Growth 163:455–460

41. Bai R, Lai Y, Zhang M, Yu F (2018) Theory and application of a novel soil freezing characteristic curve. Appl Therm Eng 129:1106–1114. https://doi.org/10.1016/j.applthermaleng.2017.10.121

42. Koopmans RWR, Miller RD (1966) Soil freezing and soil water characteristic curves. Soil Sci Soc Am J 30:680–685

43. Patterson DE, Smith MW (1981) The measurement of unfrozen water content by time domain reflectometry: results from laboratory tests. Can Geotech J 18:131–144. https://doi.org/10.1139/t81-012

44. Spaans EJ a, Baker JM (1995) Examining the use of time domain refiectometry for measuring liquid water content in frozen soil. Water Resour Res 31:2917–2925. https://doi.org/10.1029/95WR02769

45. Anderson DM, Tice AR (1973) The unfrozen interfacial phase in frozen soil water systems. In: Physical aspects of soil water and salts in ecosystems. pp 107–124

46. Kolaian JH, Low PF (1963) Calorimetric determination of unfrozen water in montmorillonite pastes. Soil Sci 95:376–384

47. Kozlowski T (2003) A comprehensive method of determining the soil unfrozen water curves. Cold Reg Sci Technol 36:71–79. https://doi.org/10.1016/S0165-232X(03)00007-7

48. Yong RN, Cheung C, Sheeran DE (1979) Prediction of Salt Influence on Unfrozen Water Content in Frozen Soils. In: Developments in Geotechnical Engineering. pp 137–155

49. Anderson DM, Hoekstra P (1965) Migration of interlamellar water during freezing and thawing of Wyoming bentonite. Soil Sci Soc Am J 29:498–504. https://doi.org/10.2136/sssaj1965.03615995002900050010x

50. Anderson DM, Morgenstern NR (1973) Physics, chemistry, and mechanics of frozen ground: a review. In: Permafrost: North American Contribution [to The] Second International Conference; National Academies: Washington, DC, USA. p 257

51. Stähli M, Stadler D (1997) Measurement of water and solute dynamics in freezing soil columns with time domain reflectometry. J Hydrol 195:352–369. https://doi.org/10.1016/S0022-1694(96)03227-1

52. Zhou X, Zhou J, Kinzelbach W, Stauffer F (2014) Simultaneous measurement of unfrozen water content and ice content in frozen soil using gamma ray attenuation and TDR. J Am Water Resour Assoc 5:2–2. https://doi.org/10.1111/j.1752-1688.1969.tb04897.x

53. Schafer H, Beier N (2020) Estimating soil-water characteristic curve from soil-freezing characteristic curve for mine waste tailings using time domain reflectometry. Can Geotech J 57:73–84. https://doi.org/10.1139/cgj-2018-0145

54. Tice AR, Anderson DM, Sterrett KF (1982) Unfrozen water contents of submarine permafrost determined by nuclear magnetic resonance. In: Developments in Geotechnical Engineering. pp 135–146

55. Li Z, Chen J, Sugimoto M (2020) Pulsed NMR Measurements of Unfrozen Water Content in Partially Frozen Soil. J Cold Reg Eng 34:04020013. https://doi.org/10.1061/(ASCE)CR.1943-5495.0000220

56. Yoshikawa K, Overduin PP (2005) Comparing unfrozen water content measurements of frozen soil using recently developed commercial sensors. Cold Reg Sci Technol 42:250–256. https://doi.org/10.1016/j.coldregions.2005.03.001

57. Topp GC, Davis JL, Annan AP (1980) Electromagnetic determination of soil water content: Measurements in coaxial transmission lines. Water Resour Reserch 16:574–582

58. Smith MW, Tice AR (1988) Measurement of the unfrozen water content of soils: comparison of NMR and TDR methods. CRREL report, 88 - 18.

59. Roth K, Schulin R, Fluhler H, Attinger W (1990) Calibration of time domain reflectometry for water content measurement using a composite dielectric approach. WATER Resour Res VOL 26:2267–2273

60. Watanabe K, Wake T (2009) Measurement of unfrozen water content and relative permittivity of frozen unsaturated soil using NMR and TDR. Cold Reg Sci Technol 59:34–41. https://doi.org/10.1016/j.coldregions.2009.05.011

61. Spaans EJA, Baker JM (1996) The Soil Freezing Characteristic: Its Measurement and Similarity to the Soil Moisture Characteristic. Soil Sci Soc Am J 60:13–19

62. Bittelli M, Flury M, Campbell GS (2003) A thermodielectric analyzer to measure the freezing and moisture characteristic of porous media. Water Resour Res 39:

63. Tian H, Wei C, Wei H, Zhou J (2014) Freezing and thawing characteristics of frozen soils: Bound water content and hysteresis phenomenon. Cold Reg Sci Technol 103:74–81. https://doi.org/10.1016/j.coldregions.2014.03.007

64. Horiguchi K, Miller RD (1980) Experimental studies with frozen soil in an “ice sandwich” permeameter. Cold Reg Sci Technol 3:177–183. https://doi.org/10.1016/0165-232X(80)90023-3

65. Kruse AM, Darrow MM (2017) Adsorbed cation effects on unfrozen water in fine-grained frozen soil measured using pulsed nuclear magnetic resonance. Cold Reg Sci Technol 142:42–54. https://doi.org/10.1016/j.coldregions.2017.07.006

66. Hu G, Zhao L, Zhu X, et al (2020) Review of algorithms and parameterizations to determine unfrozen water content in frozen soil. Geoderma 368:114277. https://doi.org/10.1016/j.geoderma.2020.114277

67. Hoekstra P (1966) Moisture movement in soils under temperature gradients with the cold-side temperature below freezing. Water Resour Res 2:241–250

68. Torrance JK, Schellekens FJ (2006) Chemical factors in soil freezing and frost heave. Polar Rec (Gr Brit) 42:33–42. https://doi.org/10.1017/S0032247405004894

69. Arenson LU, Johansen MM, Springman SM (2004) Effects of volumetric ice content and strain rate on shear strength under triaxial conditions for frozen soil samples. Permafr Periglac Process 15:261–271. https://doi.org/10.1002/ppp.498

589 70. Zhang H, Zhang J, Zhang Z, et al (2020) Variation behavior of pore-water pressure in
590 warm frozen soil under load and its relation to deformation. Acta Geotech 15:603–614.
591 https://doi.org/10.1007/s11440-018-0736-4

592 71. Darrow MM (2011) Thermal modeling of roadway embankments over permafrost. Cold
593 Reg Sci Technol 65:474–487. https://doi.org/10.1016/j.coldregions.2010.11.001

594 72. Mu QY, Zhou C, Ng CWW, Zhou GGD (2019) Stress Effects on Soil Freezing
595 Characteristic Curve: Equipment Development and Experimental Results. Vadose Zo J
596 18:1–10. https://doi.org/10.2136/vzj2018.11.0199

597 73. Ming F, Chen L, Li D, Du C (2020) Investigation into Freezing Point Depression in Soil
598 Caused by NaCl Solution. Water 12:2232. https://doi.org/10.3390/w12082232

599 74. Suzuki S (2004) Dependence of unfrozen water content in unsaturated frozen clay soil
600 on initial soil moisture content. Soil Sci Plant Nutr 50:603–606.
601 https://doi.org/10.1080/00380768.2004.10408518

602 75. Wu M, Tan X, Huang J, et al (2015) Solute and water effects on soil freezing
603 characteristics based on laboratory experiments. Cold Reg Sci Technol 115:22–29.
604 https://doi.org/10.1016/j.coldregions.2015.03.007

605 76. Jia H, Ding S, Wang Y, et al (2019) An NMR-based investigation of pore water freezing
606 process in sandstone. Cold Reg Sci Technol 168:102893.
607 https://doi.org/10.1016/j.coldregions.2019.102893

608 77. Boussaid K (2005) Sols intermédiaires pour la modélisation physique : application aux
609 fondations superficielles. École Centrale de Nantes et Université de Nantes

610 78. Ren J, Vanapalli SK (2019) Comparison of Soil-Freezing and Soil-Water Characteristic
611 Curves of Two Canadian Soils. Vadose Zo J 18:1–14.
612 https://doi.org/10.2136/vzj2018.10.0185

613 79. Ma T, Wei C, Xia X, et al (2017) Soil freezing and soil water retention characteristics:
614 connection and solute effects. J Perform Constr Facil 31:1–8.
615 https://doi.org/10.1061/(ASCE)CF.1943-5509.0000851

616 80. Wan X, Liu E, Qiu E (2021) Study on ice nucleation temperature and water freezing in
617 saline soils. Permafr Periglac Process 32:119–138. https://doi.org/10.1002/ppp.2081

618 81. Bing H, Ma W (2011) Laboratory investigation of the freezing point of saline soil. Cold
619 Reg Sci Technol 67:79–88. https://doi.org/10.1016/j.coldregions.2011.02.008

620 82. Wraith JM, Or D (1999) Temperature effects on soil bulk dielectric permittivity
621 measured by time domain refiectometry: Experimental evidence and hypothesis
622 development. Water Resour Res 35:361–369

623 83. Haynes WM (2016) CRC Handbook of Chemistry and Physics, 97th Editi. CRC press

624 84. Birchak JR, Gardner CG, Hipp JE, Victor JM (1974) High dielectric constant microwave

probes for sensing soil moisture. Proc IEEE 62:93–98. https://doi.org/10.1109/PROC.1974.9388

85. He H, Dyck M (2013) Application of multiphase dielectric mixing models for understanding the effective dielectric permittivity of frozen soils. Vadose Zo J 12:. https://doi.org/10.2136/vzj2012.0060

86. Nagare RM, Schincariol RA, Quinton WL, Hayashi M (2011) Laboratory calibration of time domain reflectometry to determine moisture content in undisturbed peat samples. Eur J Soil Sci 62:505–515. https://doi.org/10.1111/j.1365-2389.2011.01351.x

87. Zhou X, Zhou J, Kinzelbach W, Stauffer F (2014) Simultaneous measurement of unfrozen water content and ice content in frozen soil using gamma ray attenuation and TDR. Water Resour Res 50:9630–9655. https://doi.org/10.1002/2014WR015640

88. Su Y, Cui Y-J, Dupla J-C, Canou J (2022) Soil-water retention behaviour of fine/coarse soil mixture with varying coarse grain contents and fine soil dry densities. Can Geotech J 59:291–299. https://doi.org/10.1139/cgj-2021-0054

89. Fletcher NH (1970) The chemical physics of ice. Press Cambridge, Engl 111

90. Y.Uzu, Sano I (1965) On the Freezing of the Droplets of Aqueous Solutions. J Meteorol Soc Japan Ser II 43:290–292

91. Yershov ED (2004) General Geocryology. Cambridge University Press

92. Banin A, Anderson DM (1974) Effects of Salt Concentration Changes During Freezing on the Unfrozen Water Content of Porous Materials. Water Resour Res 10:124–128

93. Han Y, Wang Q, Kong Y, et al (2018) Experiments on the initial freezing point of dispersive saline soil. Catena 171:681–690. https://doi.org/10.1016/j.catena.2018.07.046

94. Cannell GH, Gardner WH (1959) Freezing-point depressions in stabilized soil aggregates, synthetic soil, and quartz sand. Soil Sci Soc Am J 23:418–422. https://doi.org/10.2136/sssaj1959.03615995002300060018x

95. Kozlowski T (2016) A simple method of obtaining the soil freezing point depression, the unfrozen water content and the pore size distribution curves from the DSC peak maximum temperature. Cold Reg Sci Technol 122:18–25. https://doi.org/10.1016/j.coldregions.2015.10.009

96. Wen Z, Ma W, Feng W, et al (2012) Experimental study on unfrozen water content and soil matric potential of Qinghai-Tibetan silty clay. Environ Earth Sci 66:1467–1476. https://doi.org/10.1007/s12665-011-1386-0